THE JOURNAL OF PHYSICAL CHEMISTRY B

Article

pubs.acs.org/JPCB

cis Influence in Models of Cobalt Corrins by DFT and TD-DFT Studies

Isabelle Navizet,*[,†] Christopher B. Perry,*[,†] Penny P. Govender,[†,‡] and Helder M. Marques[†]

[†]Molecular Sciences Institute, School of Chemistry, University of Witwatersrand, P.O. Wits, Johannesburg, 2050 South Africa

[‡]Department of Applied Chemistry, University of Johannesburg, P.O. Box 17011, Doornfontein, Johannesburg, 2028 South Africa

ABSTRACT: Time-dependent density-functional theory and density-functional theory are applied to study the cis influence of the equatorial macrocycle in vitamin B_{12} derivatives. A series of dicyanocobalt corrinoids, CN-[Co(III)-corrin]-CN, where the $C_{10}H$ of the corrin ring is replaced by different substituents, X, is considered. The calculated UV−visible absorption spectra, the charge distribution obtained from a Bader QTAIM analysis of the electron density, the CN stretch frequencies of the axial cyano ligands and the electron densities at some bond critical points are compared. The main absorption bands in the UV−visible spectra depend on the electron donating or withdrawing power of X, as assessed from its Hammett σ_p constants. For X with a stronger electron donating power than H, the other properties do not change appreciably. However, when $\sigma_p(X) > \sigma_p(H)$, these properties vary linearly with the electron withdrawing power of the substituent. This helps explain the experimental observation that substitution of the axial ligand is more difficult and proceeds more slowly with the increase of the electron withdrawing power of the C_{10} substituent.

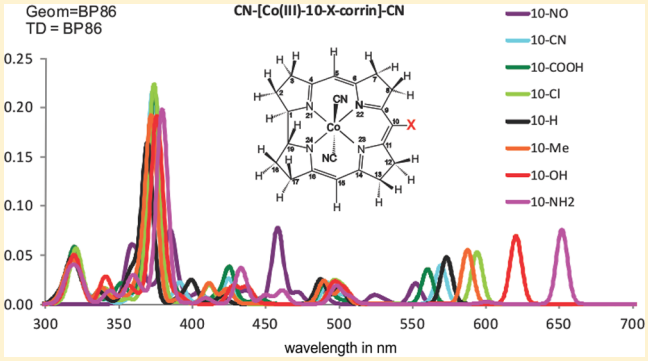

1. INTRODUCTION

Vitamin B_{12} derivatives are important cofactors involved in a number of enzymatic reactions in various organisms.[1] The common pharmaceutical form of vitamin B_{12} is cyanocobalamin (CNCbl). This form is converted in the body into two biologically active forms of vitamin B_{12}, 5′-deoxyadenosylcobalamin (AdoCbl) and methylcobalamin (MeCbl). In cobalamin complexes, the cobalt central ion is formally in the +3 oxidation state. It is coordinated in the equatorial (cis) plane by the nitrogen atoms of the corrin ring and axially by two other ligands (the α and β ligands). The lower or α ligand in the cobalamins is a 5,6-dimethylbenzimidazole (DBI), connected to the corrin ring at its C_{17} position (see Figure 1).

In vitamin B_{12} derivatives, Co(III) is unusually labile toward axial ligand substitution compared to other Co(III) complexes. It has been proposed[2−4] that this is due to the cis-labilizing influence of the corrin ring, i.e., that there is some transfer of electron density from the equatorial corrin ring to the axial coordination site of Co(III) which imparts some labile Co(II)-like character on the metal center.

The cis influence can be investigated in two ways: (i) what is the influence of the nature of the β ligand on the properties of the corrin ring? and (ii) what is the influence of the nature of the corrin ring on the properties of the β ligand?

The second question has been addressed.[5] It was noted that the approximate lability ratio of the second-order rate constants for substitution of H_2O by an exogenous ligand, L, in Co(III) octahedral complexes containing four N-donor equatorial ligands is 10^9:10^6:10^4:1 for corrin, porphyrin, cobaloxime, and amine systems, respectively. These systems differ in several ways:

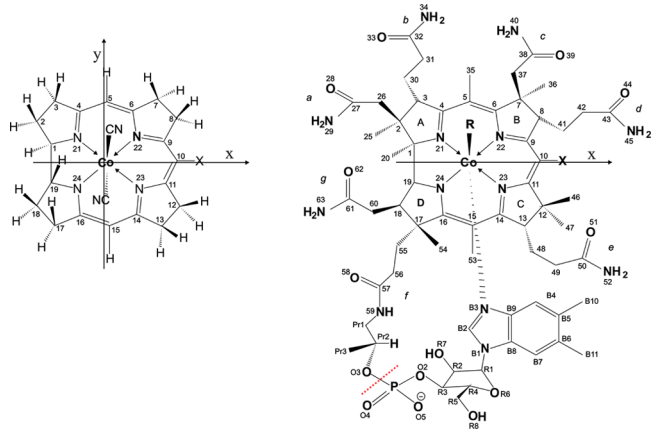

Figure 1. Structure of vitamin B_{12} derivatives and numbering of the corrin ring. Cobalamin structures (right) have the nucleotide tail as the α ligand. R is the β ligand. R = CN, cyanocobalamin (vitamin B_{12}) CNCbl; R = H_2O aquacobalamin H_2OCbl^+ ; R = CH_3 methylcobalamin MeCbl. Cobinamide lacks the dimethylbenzimidazole nucleotide tail. In this case, the f tail is cut after the dashed red line. The dicyano corrin model used for the calculations presented in this work is shown on the left.

the size of the cavity in which the metal is encapsulated, the extent of conjugation of the equatorial ligand system, and the charge on that system. It is unlikely that any one of these

Received: April 25, 2012
Revised: June 25, 2012
Published: June 25, 2012

   dx.doi.org/10.1021/jp304007a | *J. Phys. Chem. B* 2012, 116, 8836−8845

properties, taken individually, can explain the general trend. Thus, only the corrin and the porphyrin are macrocycles; the corrin macrocycle carries a −1 charge, whereas the porphyrin carries a −2 charge; cobaloximes are less extensively conjugated than corrins, whereas corrins are less extensively conjugated than porphyrins; the cavity in a corrin is considerably smaller than that in a porphyrin, whereas there is limited and no restriction, respectively, to the cavity size in cobaloximes and tetrammine systems.

By replacing the H at C_{10} of the corrin ring by different substituents X or changing the β-ligand Y, both the influence of X on the properties of Y and the influence of Y on the C_{10}-X properties can be investigated. This issue has been experimentally investigated in the case of the substitution of H at C_{10} by Cl in YCbl (Y = aqua, methyl, or cyano) derivatives[4,5] or by NO in H_2OCbl^+.[2]

First, the electron donor power of Y, i.e., the capacity to donate electron density to the rest of the molecule, increases in the order Me < CN < H_2O. X-ray diffraction data showed that there is a corresponding increase in the length of the C_{10}−Cl bond with an increase in the donor power of Y.[5] Second, replacing the H at C_{10} by a strongly electron-withdrawing NO group deactivates the metal ion toward ligand substitution.[2] A comparison of the equilibrium constants for the substitution of Y = H_2O in 10-Cl-H_2OCbl^+ and H_2OCbl^+ shows that anionic ligands bind more strongly to H_2OCbl^+ than to 10-Cl-H_2OCbl^+ while this is the converse for neutral ligands.[4] The same study also showed that the kinetics for the reaction of 10-Cl-H_2OCbl^+ with pyridine and N_3^- are slower than for H_2OCbl^+ and that the pK_a of coordinated H_2O at 25 °C drops from 8.09 in H_2OCbl^+ to 7.65 in 10-Cl-H_2OCbl^+. Semiempirical molecular orbital calculations on the hydroxo complexes show that charge density is delocalized from the axial O-donor atom to Co and Cl, thus explaining why coordinated OH^- is a poorer base in 10-Cl-HOCbl than it is in HOCbl. Third, the substitution of H at C_{10} by Cl causes the bands in the electronic spectrum of 10-Cl-YCbl (Y = aqua, methyl or cyano) derivatives to shift to lower energies, consistent with an increase in the electron density in the corrin ring.[5] Again, the electronic transitions of the cobalamins shift to lower energies as the donor power of the axial ligand Y increases. Moreover, this cis influence correlates with the trans influence, as the Co−N bond length to the trans dimethylbenzimidazole ligand of the corrins decrease with the increase of the donor power of the axial ligand Y.[6] All of these observations provide convincing evidence that the axial ligands and the corrin macrocycle are in electronic communication.

The electronic absorption spectra of cobalamins are influenced both by the oxidation state of the metal and the nature of the axial ligands. Traditionally, all observed electronic transitions for Co(III) cobalamins have primarily been attributed to $\pi \rightarrow \pi^*$ transitions of the corrin ring.[7] The absorption spectra of CNCbl and H_2OCbl^+ (commonly referred to as "typical" or "normal" cobalamin spectra[8]) are dominated by two features, the α/β bands in the visible region, and the γ band in the near-UV region. The absorbance spectra of alkylcobalamins (such as MeCbl and AdoCbl, referred to as "atypical", "unique", or "anomalous" spectra) have a γ band that is strikingly different to that observed for CNCbl and H_2OCbl^+. The γ band is less intense, and is composed of several transitions in the UV region.[8,9] Based on Gaussian deconvolution of the absorption spectra, it has been suggested that there is no fundamental difference between the "typical" and "atypical" spectra of the cobalamins and that the difference in appearance arises merely from the relative positions of the components of the spectrum that make up the γ-region.[6]

Time dependent density functional theory (TD-DFT)[10,11] is arguably the most practical computational method that can routinely be used to study the excited states of large and complex molecules.[12] The excited states of various cobalamin derivatives have already been modeled with TD-DFT methods.[13−23]

Andruniow et al.[15] first reported the use of TD-DFT in conjunction with the B3LYP hybrid functional to analyze the electronic absorption spectra of cyanocobalamin models, CN-[Co(III)-corrin]-CN and CN-[Co(III)-corrin]-imidazole. Their study was a significant improvement on previous attempts using semiempirical methods.[24,25] Their results show that the energies of the transitions agree well with the experimental spectrum after uniformly scaling the transitions by ∼0.5 eV, chosen such that the apparent position of the γ band coincides with that observed experimentally.

Brunold and co-workers[21] measured the absorbance, circular dichroism (CD), magnetic CD (MCD), and resonance Raman spectra of a representative set of cob(III)alamin species. They analyzed their experimental results by comparing them with TD-DFT calculations of the absorbance spectra. Their results show that the "unique" spectra of alkylcobalamins do indeed differ from the "typical" spectra of H_2OCbl^+ and CNCbl; the key difference in going from H_2OCbl^+ to MeCbl is a significant increase in the number of occupied MOs near the HOMO. These orbitals have Co metal character and some of them methyl $2p_z$ character. The net effect is that transfer of electron density from the alkyl ligand to the metal center lowers the effective charge Z_{eff} of the metal and raises the energies of all the metal 3d orbitals. A second key finding is that the transition responsible for the α/β bands in CNCbl and H_2OCbl^+ primarily involves a single HOMO → LUMO excitation, corresponding to the α band, with the β band being the first member of a vibrational progression. In the case of MeCbl, there are two transitions in the α/β region. However, a recent report by Kozlowski et al.[20] involving a reinvestigation of the absorbance, CD, and MCD spectra of CNCbl and MeCbl using TD-DFT shows that the α/β bands of CNCbl, as well as that of MeCbl, arise from multiple transitions, thus disputing previous hypotheses that the bands originate from a single electronic excitation. The authors do note however, that TD-DFT simulated absorbance spectra are very sensitive to the type of functional used; very different assignments regarding the number of electronic transitions that comprise the α/β band have been made based on the type of functional used.[13−15,17,19−21] The consensus from all of these studies points toward the BP86 functional as the most reliable functional for reproducing the experimental cobalamin absorbance spectra. A recent benchmark analysis shows that the GGA type functionals (such as BP86) are more appropriate than hybrid functionals.[26]

In the present contribution, we further examine the cis-influence in cobalamin chemistry by calculating and analyzing the absorption spectra of model C_{10}-substituted cobalt(III) corrin systems in which the H at C_{10} is substituted with a variety of electron-donating and electron-withdrawing groups. The central questions we have sought to answer are (i) whether the electron distribution in the system and in the corrin in particular changes with the nature of the C_{10} substituent and (ii) does the ionicity of the axial bond depend on the nature of the C_{10} substituent? All results are obtained within the framework of DFT, TD-DFT, and Bader's quantum theory of atoms in molecules (QTAIM) approach.[27]

dx.doi.org/10.1021/jp304007a | J. Phys. Chem. B 2012, 116, 8836−8845

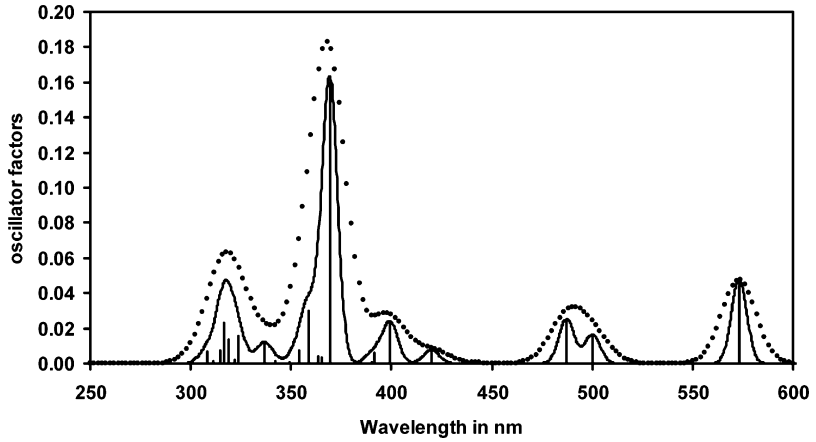

Figure 2. Simulated electronic absorption spectrum of CN-[Co(III)-corrin]-CN based on the 30 first singlet excited states computed at the optimized ground-state geometry at the TD-DFT/BP86/6-31+G(d,p) level. The solid line corresponds to a Doppler broadening with a width at half peak of 9 nm and the dotted line corresponds to a Doppler broadening with a width at half peak of 20 nm. These data were obtained with Chemcraft.[42]

2. COMPUTATIONAL METHODS

All DFT calculations were performed using Gaussian 09[28] on a dicyano-Co(III) corrin system CN-[Co(III)-corrin]-CN in which all substituents of the corrin, with the exception of the C_{10} substituent, were replaced by H (Figure 1). The starting geometry was generated from the crystal structure of heptamethyl dicyano-cobyrinate[29] by replacing all corrin substituents with H atoms, and the H at C_{10} with a variety of electron-donating and electron-withdrawing groups.

For each derivative, full geometry optimizations were performed using a 6-31+G(d,p) basis set and, in some cases, the larger triple-ζ 6-311+G(d,p) basis set for validation purposes. The BP86 functional has been shown to be the most reliable one for reproducing the coordination sphere geometrical parameters of cobalt corrinoids[30−32] and was hence used for all geometry optimizations. Previous calculations have shown that simulated absorption spectra depend strongly on the nature of the functional used;[13,14,17,19,20] we have thus calculated vertical excitation energies for all C_{10}-derivatives at their optimized BP86 geometries using the BP86 and for comparison, in the case of the nonsubstituted compound, CAM-B3LYP,[33] M06,[34,35] B3LYP,[36−39] and PBE1PBE[40−42] functionals. Thirty singlet excited states proved to be sufficient for reproducing the main features of derivatives whose experimental electronic absorption spectra are available. Spectra and orbital visualization was with Chemcraft.[43]

The wave function files required for the analysis of the topological properties of the electron density using the atoms in molecules (AIM) framework of Bader[27] were generated using the BP86/6-31+G(d,p) optimized geometries by performing a single-point calculation at the same level of theory. The topological properties of the electron density ($\rho(r)$), its Laplacian ($\nabla^2 \rho(r)$), the potential energy density ($V(r)$), the kinetic energy density ($G(r)$), and the total energy densities ($H(r)$) were evaluated at all of the bond critical points (bcp's), ring critical points (rcp's), and cage critical points (ccp's) using the AIMALL and AIM2000 suite of programs.[44,45]

3. RESULTS AND DISCUSSION

3.1. UV−Visible Absorption Spectra of CN-[Co(III)-Corrin]-CN. Figure 2 shows the TD-DFT BP86 spectra obtained from the calculation of the first 30 excited states of CN-[Co(III)-corrin]-CN. The "typical" spectrum of cyanocobalamin can be recognized by an α band near 580 nm and a γ band near 370 nm.

The calculated spectrum may be compared to that reported for dicyano-cobinamide by Firth et al.[9] in 1967 (see Figure 1 for structure) and the spectrum of dicyano-Co(III)-(7,7,12,12,19)-pentamethyl-corrin by Eschenmoser et al. in 1965.[46] In the latter, the authors compare the spectra of dicyano-cobalt pentamethyl corrin with that of dicyano-Co(III)heptamethyl cobyrinoate (cobester), a derivative of the cobinamide structure in which all amide groups are replaced by methyl esters and where all eight methyl groups of the corrin are present. The principal bands of the cobester are red-shifted compared to the spectrum of the cobalt pentamethyl corrin, which the authors attributed to the two extra methyl groups bound at C_5 and C_{15}. A close examination of their spectra shows that the band shifts are not the same; the presence of the C_5 and C_{15} Me groups causes a red shift of 20 nm for the γ band, but a larger red shift, 33 nm, for the α band (Table 1).

Table 1. Principal Peaks in the Experimental UV−Visible Spectra of Substituted Dicyano Co(III) Corrins

	wavelength/nm			
corrinoid	γ	β	α	ref
dicyano-cobalamin (C_{10}−H)	367	550	580	47
dicyano-aminocobalamin (C_{10}-NH_2)	379	610	655sh[a]	47
dicyano-chlorocobalamin (C_{10}-Cl)	369	561	602	48
dicyano-bromocobalamin (C_{10}-Br)	370	561	602	47
dicyano-nitrosocobalamin (C_{10}-NO)	354	415sh[a]	530	47
	356	530	568	17
dicyanocobinamide	368	542	583	9
CN-[Co(III)-pentamethylcorrin]-CN	349	511	549	46
dicyanoheptamethylcobyrinoate	369	541	582	46

[a]shoulder.

We performed a calculation on CN-[Co(III)-5,15-dimethyl-corrin]-CN and compared its predicted spectrum to that of the dicyano corrin in which H rather than Me was present at C_5 and C_{15}; we observed a red shift of 3 nm for the γ band and one of 10 nm for the α band. This is the same trend as observed experimentally and confirms that the red shift of the bands is indeed due to the presence of Me groups at C_5 and C_{15}.

dx.doi.org/10.1021/jp304007a | J. Phys. Chem. B 2012, 116, 8836−8845

The calculated BP86 CN-[Co(III)-corrin]-CN spectrum shows a small blue shift (7 nm) for the α band and a small red shift (2 nm) for the γ band when compared with the experimental spectrum of dicyanocobalamin (Table 1). Both shifts are greater and toward the red (24 and 20 nm, respectively) when compared with the experimental spectrum of CN-[Co(III)-pentamethylcorrin]-CN. The experimental gap between the two bands is smaller in the case of the pentamethylcorrin (200 nm) than in the cobalamin (213 nm) and is closer to the gap found in the calculation (204 nm). Therefore, no scaling was done on the calculated spectra as the results are in good agreement with the cobalamin experimental data.

By comparison, other functionals give $\alpha-\gamma$ gaps that are much smaller than the experimental results. The gap is 155 nm for CAM-B3LYP, 158 nm for PBE1PBE, 159 nm for M06, and 167 nm for B3LYP. Therefore all further results presented are for the BP86 functional and without any scaling.

Only 30 singlet states were calculated as we are interested in the spectra in the α and γ regions. We found that singlet−triplet transitions have zero transition moment (oscillator strength null), so the triplets were not included in the calculations. At the Franck−Condon region, two triplet excited states are below the first singlet excited state. These triplet states are possibly involved in the photodissociation of Co−C bond[22] but are not relevant for the calculation of the absorption spectra.

We observed that the α band of the simulated spectra corresponds to the transition between the HOMO and the LUMO. The frontier molecular orbitals are presented in Figure 3. The HOMO orbital is a π orbital located on the four equatorial N atoms and on C_5, C_{10}, and C_{15} of the corrin ring, coupled with the σ orbital of the axial CN ligand. The LUMO orbital is essentially a π^* orbital of the corrin ring with some admixture of the d_{yz} orbital of cobalt (see Figure 1 for the orientation of the axes).

The α band corresponds mainly to a $(\pi_{ring}/\sigma_{CN}) \rightarrow (\pi_{ring}^*/3d_{yz})$ transition (see Table 2 state 1); thus, the band shows electron density shift from axial ligand to the corrin ring, as reported previously in ref 15. The γ band corresponds principally to an admixture of HOMO-4 → LUMO, HOMO-1 → LUMO and HOMO → LUMO+2 excitations (state 12 in Table 2). In addition to the π_{ring} character, the HOMO-4 orbital has some Co $d_{x^2-y^2}$ and CN π_y character and the HOMO-1 orbital has some Co d_{yz} and CN π_y character. The LUMO+2 orbital is a Co d_{xz} and corrin π^* orbital. Thus the characteristic of the γ band is therefore an axial ligand to equatorial corrin ring electronic transfer.

We note that the present dicyano complex has two identical axial ligands. When the axial ligands are not the same as in Im-[Co(III)-corrin]-Et^+, Im-[Co(III)-corrin]-Me^+,[22] or Im-[Co(III)-corrin]-CN^+ and DBI-[Co(III)-corrin]-CN^+,[19] the character of the orbitals involved in the transitions might change, especially when the molecular orbital's electron density is located on the axial ligand. The σ electronic density on the CN in the HOMO orbital is also found in Im-[Co^{III}-corrin]-CN^+ and DBI-[Co^{III}-corrin]-CN^+.[19]

The BP86 simulated spectrum also shows some less intense transitions between the α and γ bands. The two transitions at 500 and 487 nm (states 3 and 4 in Table 2) correspond to HOMO-1 → LUMO and HOMO-2 → LUMO transitions, respectively. The HOMO-2 has Co d_{xz} and CN π_x character, with very little electron density on the corrin ring. These two transitions therefore correspond to charge transfer from the axial ligand to the equatorial corrin ligand. These two peaks do not appear in the experimental spectrum (or may be buried beneath the α/β bands; they are also not in the simulated spectra we obtained with other functionals). They might be so-called ghost states,[49] states that are red-shifted from wavelengths shorter than the γ band to longer wavelengths because of the use of a pure density functional for these charge transfer character states.

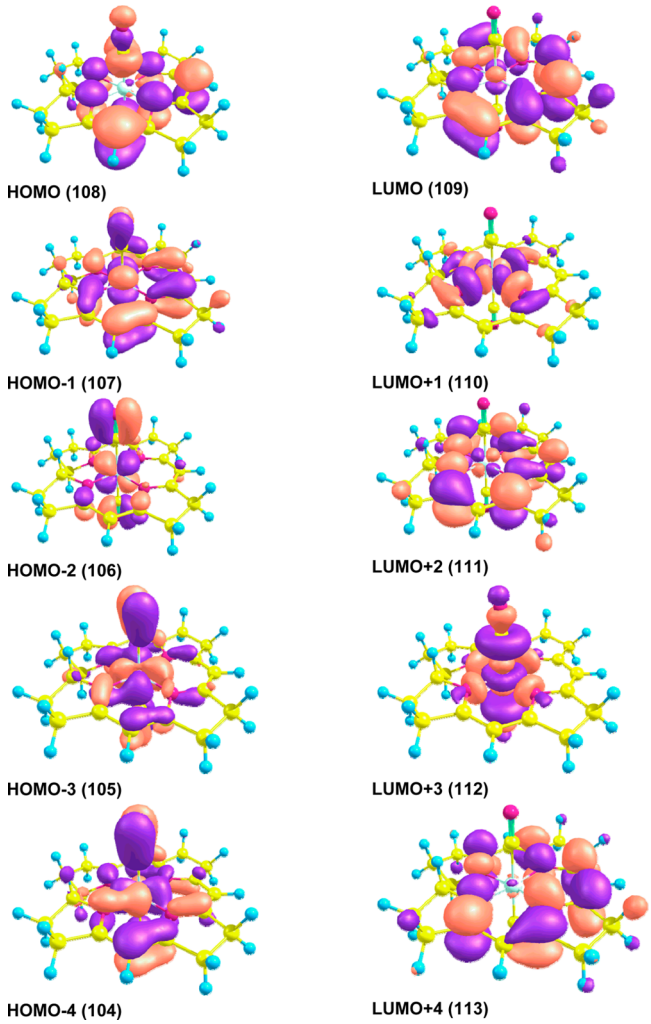

Figure 3. Principal molecular orbitals of CN-[Co(III)-corrin]-CN at TD-DFT/BP86/6-31+G(d,p) level.

The origin of the β band is still not resolved by our calculation. In the experimental spectra, there are several peaks found in the α/β band region. They have been interpreted as a vibrational progression due to the change along the normal mode of the corrin stretching vibration.[16,50] The present BP86 simulated spectrum of CN-[Co(III)-corrin]-CN gives no electronic transition that explains the β band, as the one calculated by Andruniow et al. for the same compound,[15] and in contrast to the one of Me-[Co(III)-corrin]-Im^+ calculated by the same authors.[13] The present spectrum is thus suggestive of the presence of a vibrational progression, in line with the results on structural and electronic properties of dicyano- and aqua-cyanocobester.[17]

3.2. UV−Visible Absorption Spectra for C_{10} Substituted Corrins. The simulated absorption spectra of dicyano cobalt corrin compounds substituted at C_{10} are shown in Figure 4. We have chosen a range of substituents X from a strongly electron donating ($-NH_2$) group to a strongly electron withdrawing

dx.doi.org/10.1021/jp304007a | J. Phys. Chem. B 2012, 116, 8836−8845

Table 2. TD-DFT/BP86 Wavelength (λ), the Corresponding Oscillator Strenghts (f), and Description of the Dominant Configuration for the CN-[Co(III)-corrin]-CN Complex[a]

state	λ(nm)	f	transition	%	donor MO	acceptor MO
1	573.19	0.0475	108 → 109	94	π_{ring}/σ_{CN}(HOMO)	π_{ring}*/$3d_{yz}$(LUMO)
3	500.15	0.0165	107 → 109	82	$\pi_{ring}/\pi_{yCN}/3d_{yz}$(HOMO-1)	π_{ring}*/$3d_{yz}$(LUMO)
4	487.26	0.0252	106 → 109	93	$\pi_{xCN}/3d_{xz}$(HOMO-2)	π_{ring}*/$3d_{yz}$(LUMO)
8	399.39	0.0232	108 → 112	96	π_{ring}/σ_{CN}(HOMO)	σ_{CN}*/d_{z^2}(LUMO+3)
12	369.31	0.1598	104 → 109	34	$\pi_{ring}/\pi_{yCN}/3d_{x^2-y^2}$(HOMO-4)	π_{ring}*/$3d_{yz}$(LUMO)
			107 → 109	10	$\pi_{ring}/\pi_{yCN}/3d_{yz}$(HOMO-1)	π_{ring}*/$3d_{yz}$(LUMO)
			108 → 111	35	π_{ring}/σ_{CN}(HOMO)	π_{ring}*/$3d_{xz}$(LUMO+2)
16	358.77	0.0297	102 → 109	18	π_{xCN}(HOMO-6)	π_{ring}*/$3d_{yz}$(LUMO)
			103 → 109	53	π_{ring}/π_{CN}(HOMO-5)	π_{ring}*/$3d_{yz}$(LUMO)
			108 → 113	17	π_{ring}/σ_{CN}(HOMO)	π_{ring}*(LUMO+4)
21	336.53	0.0117	104 → 111	14	$\pi_{ring}/\pi_{yCN}/3d_{x^2-y^2}$(HOMO-4)	π_{ring}*/$3d_{xz}$(LUMO+2)
			105 → 111	15	$\pi_{yCN}/3d_{x^2-y^2}$(HOMO-3)	π_{ring}*/$3d_{xz}$(LUMO+2)
			106 → 112	40	$\pi_{xCN}/3d_{xz}$(HOMO-2)	σ_{CN}*/d_{z^2}(LUMO+3)
			108 → 113	16	π_{ring}/σ_{CN}(HOMO)	π_{ring}*(LUMO+4)
22	323.59	0.0154	104 → 111	31	$\pi_{ring}/\pi_{yCN}/3d_{x^2-y^2}$(HOMO-4)	π_{ring}*/$3d_{xz}$(LUMO+2)
			105 → 111	19	$\pi_{yCN}/3d_{x^2-y^2}$(HOMO-3)	π_{ring}*/$3d_{xz}$(LUMO+2)
			106 → 112	12	$\pi_{xCN}/3d_{xz}$(HOMO-2)	σ_{CN}*/d_{z^2}(LUMO+3)
			108 → 113	12	π_{ring}/σ_{CN}(HOMO)	π_{ring}*(LUMO+4)
24	318.84	0.0137	107 → 113	83	$\pi_{ring}/\pi_{yCN}/3d_{yz}$(HOMO-1)	π_{ring}*(LUMO+4)
25	316.56	0.0232	102 → 110	85	π_{xCN}(HOMO-6)	$\sigma_{Co\text{-}Nring}$*/d_{xy}(LUMO+1)

[a]Only contributions of dominant one-electron excitation greater than 10% and only states with f value greater than 0.01 are reported.

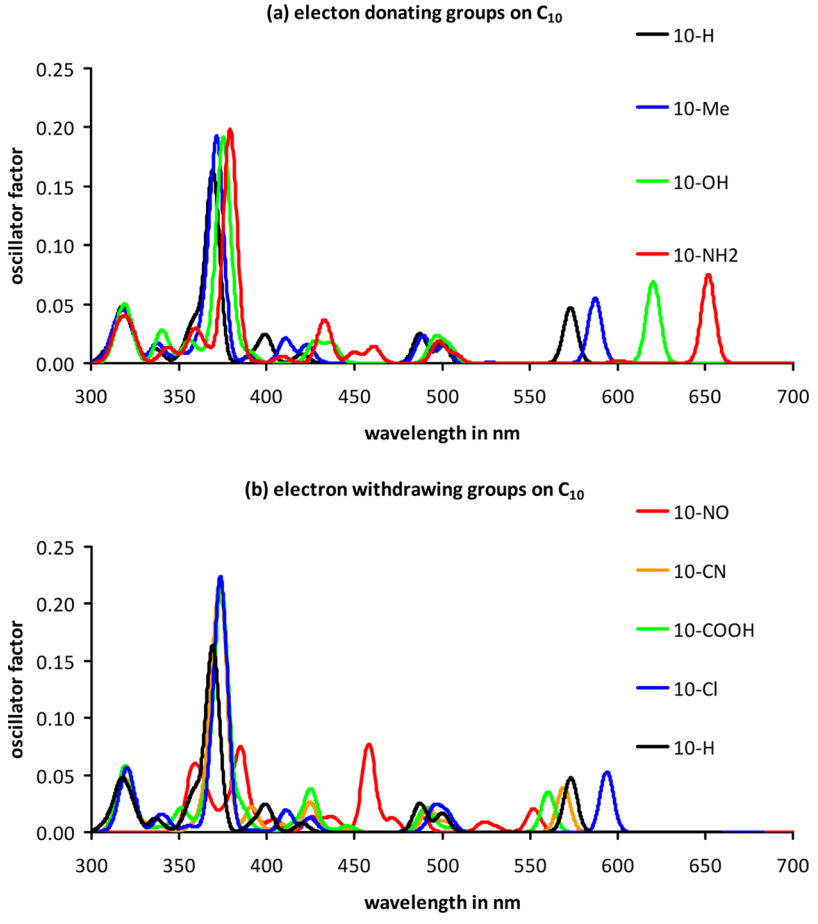

Figure 4. Simulated electronic absorption spectra of C_{10}-subtituted corrins. (a) Calculated spectra for electron donating X groups ($\sigma_p < 0$). (b) Calculated spectra for electron withdrawing X groups ($\sigma_p > 0$).

(−NO) group. We have used the Hammett para constants[51] σ_p to quantify the influence of the substituent (Table 3).

Except in the case of the halogens, all α bands of compounds where X is electron withdrawing are blue-shifted compared to the

dx.doi.org/10.1021/jp304007a | J. Phys. Chem. B 2012, 116, 8836−8845

Table 3. Hammett Para Constants[51] σ_p Used in This Work

X	σ_p	X	σ_p	X	σ_p
NO	0.91	Br	0.23	Me	−0.17
NO_2	0.78	Cl	0.23	OH	−0.37
CN	0.66	H	0.00	NH_2	−0.66
COOH	0.45	Benz	−0.01		

band of C_{10}-H compound and all α bands when X is electron donating are red-shifted (Figure 4). Halogens are a special case; their σ_p values are positive, placing these substituents in the group of σ withdrawing substituents, but they also have π donor character toward the π system of the corrin. This explain the red shift observed in the Figure 4b and the experimental results[5] discussed in the Introduction.

The position of the α band correlates reasonably well with the Hammett constant of the C_{10} substituent (Figure 5a; $r^2 = 0.72$, $p = 0.001$) and shifts to longer wavelength as electron donation increases. There is also a reasonable correlation between σ_p and the HOMO−LUMO gap (Figure 5c; $r^2 = 0.75$, $p = 0.0011$) provided the value for C_{10}-NO is omitted. In this latter compound, the α band corresponds to a HOMO-1 → LUMO and a HOMO-2 → LUMO transition and not to the HOMO → LUMO transition as in the others, the HOMO orbital being exclusively located on the NO substituent.

The results are readily understood on the basis of the electron density of the HOMO and LUMO. As mentioned above, both the HOMO and LUMO have corrin π character; however, the HOMO has significant electron density located on the C_{10} atom, as well as on X, whereas the electron density on these positions is low in the LUMO. For electron donors such as OH, the electron density of the HOMO has two negative overlapping π orbitals on the C_{10} and on the oxygen of the OH (Figure 6); there is locally an antibonding character, which destabilizes the MO. On the other side of the Hammett scale, for the C_{10}-CN structure, there is negligible density on the carbon atom of the CN substituent. This gives a less repulsive character to the HOMO (Figure 6) and consequently lowers the energy of the HOMO. As the LUMO is not significantly affected by the C_{10} substituent, the value of the HOMO−LUMO gap, and consequently the position of the α band, is thus affected. In summary, when X is an electron donor (negative Hammett constant) the HOMO is destabilized, the HOMO−LUMO gap decreases, and the α band shifts to longer wavelengths (Figure 4).

The influence of the substitution at the C_{10} position on the γ band is much smaller (Figures 4 and 5b) and the difference in the band position spans about 10 nm compared to the ca. 100 nm for the α band. We again find anomalous behavior for C_{10}-NO; the orbitals involved in the γ band states are not symmetric or antisymmetric with respect to the x axis as for the other compounds. Consequently, the states could not be readily compared with those of other compounds in our series.

As already stated (see above) for C_{10}-H, the γ band is an admixture of different transitions. The transitions involve orbitals which do not show any density on C_{10} such as HOMO-4, LUMO, and HOMO-1, or orbitals which has the same kind of density on C_{10} (HOMO and LUMO+2). This explains the very small influence of the C_{10} substitution on the γ band (Figure 5b).

3.3. Partial Charges. The partial charges on the complexes were calculated from a QTAIM analysis of the optimized BP86 structures. Figure 7 shows the average partial charges on the C and N atoms of the CN ligands and of Co as a function of the σ_p value of the C_{10} substituent. As electron donation from the

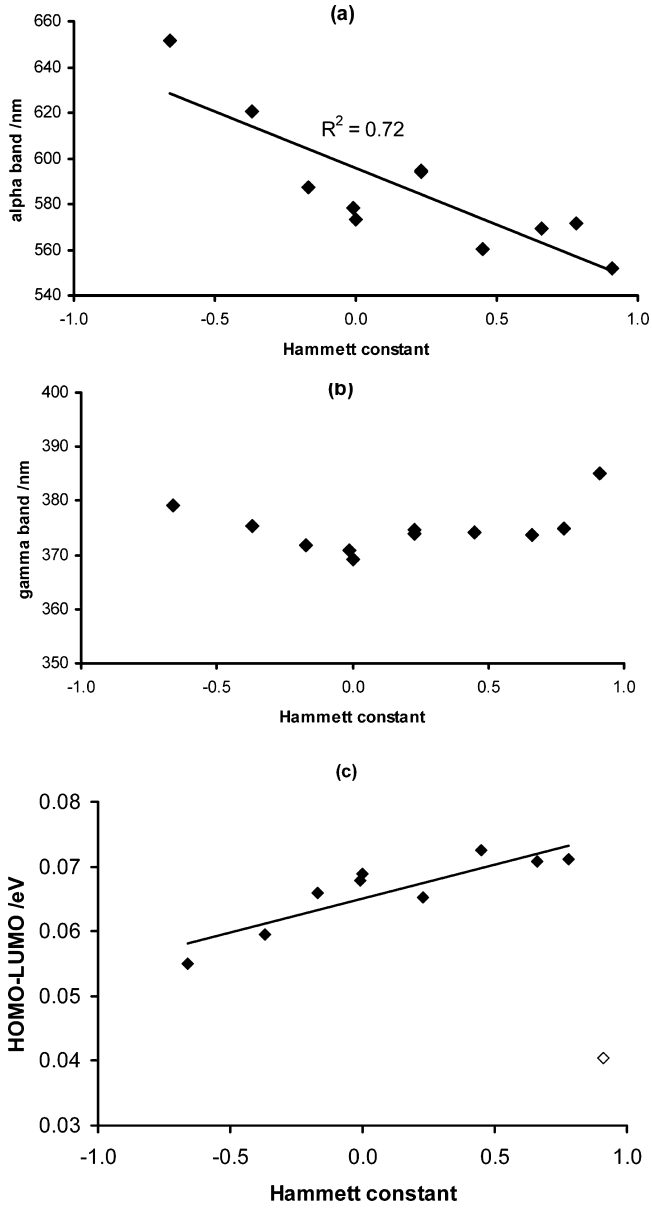

Figure 5. Dependence of the α band (a) and the γ band (b) on the σ_p value of the substituent X at C_{10}. Correlation between HOMO−LUMO gap and σ_p (c). In panel c, the value corresponding to X = NO is emphasized by an empty diamond.

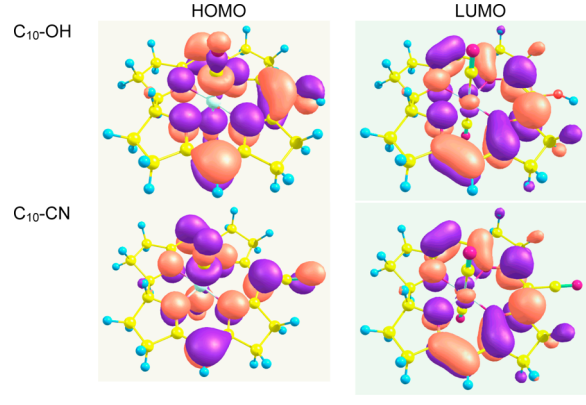

Figure 6. HOMO and LUMO of two substituted dicyano-Co(III) corrins, C_{10}-OH, and C_{10}-CN.

dx.doi.org/10.1021/jp304007a | J. Phys. Chem. B 2012, 116, 8836−8845

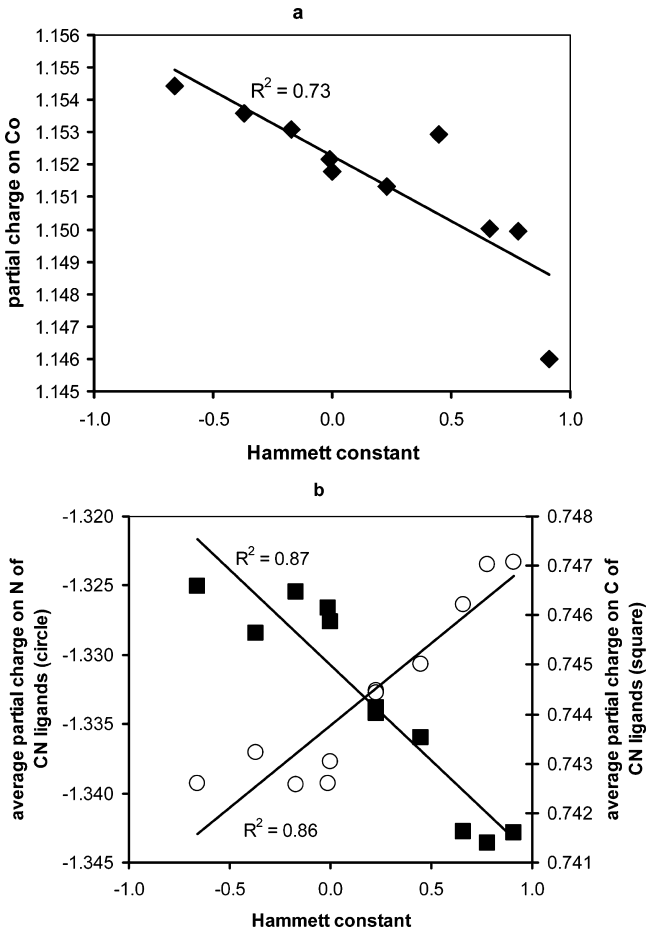

Figure 7. Partial charges on (a) Co and on (b) the C (■, right-hand axis) and N (○, left axis) of the CN ligands (average on the two CN ligands) versus the Hammett constant of the C_{10} substituent.

substituent increases, the charge on C and Co becomes more positive while that on N atom becomes more negative; the correlations are strong (C, $r^2 = 0.87$, $p < 0.01$; N, $r^2 = 0.86$, $p < 0.01$; Co, $r^2 = 0.73$, $p = 0.008$). This suggests that the ionic character of the NC-Co-CN system increases as electron donation from the C_{10} substituent increases. Interestingly, this would imply that in an N−Co−OH_2 corrin system the Co−OH_2 bond will become more ionic, i.e., H_2O should be more labile toward substitution. It is an intriguing possibility that this could be the origin of the cis-labilizing effect of the corrin. This is in line with the results obtained by the substitution of C_{10}-H by Cl discussed in the Introduction. Our results show that the ionicity of the NC-Co-CN decreases in the C_{10}-Cl compound, where the experimental results show that the lability of the 10-Cl-H_2OCbl$^+$ decreases.[4]

The total partial charge on the CN ligand, obtained by summing of the charges on C and N as a function of the C_{10} σ_p value is shown in Figure 8. There are clearly two trends. The total partial charge on CN is almost invariant with σ_p for $\sigma_p < 0$, but increases linearly, becoming less negative, with σ_p for $\sigma_p > 0$. While less obvious, similar trends are found in the individual charges on C and N (Figure 7a,b). Hence, when substituents are more electron donating than hydrogen, the charges are independent of σ_p, but when the substituents are more electron withdrawing, the ionic character of the NC-Co-CN system decreases.

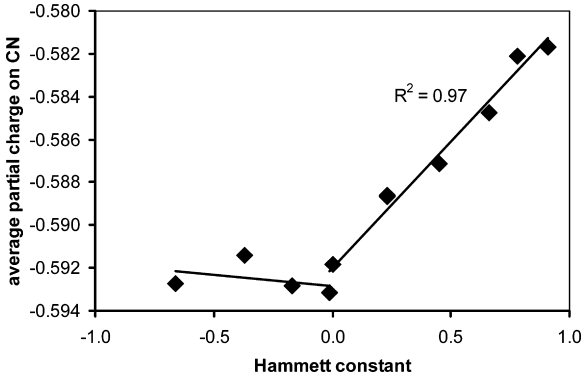

Figure 8. Dependence of the total partial charge on the CN ligands (average on the two CN ligands) as a function of the σ_p value of the C_{10} substituent.

3.4. Cyanide Stretching Frequencies. The cyanide ligand is unusual in that the frequency of its C≡N stretch, ν_{CN}, increases on coordination to a metal ion.[52−54] As the donor power of the α ligand, trans to CN^- in a cobalt corrin, increases, ν_{CN} decreases and may approach the stretching frequency of free cyanide (reported at between 2078 and 2080 cm^{-1}).[55,56] The frequency ν_{CN} of solid KCN have been measured at 2078 cm^{-1}.[17] The stretching frequency of coordinated cyanide provides a good example of the trans influence in cobalamin chemistry; thus, ν_{CN} = 2130, 2119, 2088, and 2083 cm^{-1} when the trans ligand is H_2O, CN^-, methyl, and *n*-propyl, respectively.[57] There is also evidence for the cis influence of the macrocycle. For example, ν_{CN} in trans dicyanides CN-[Co^{III}-L]-CN occurs at 2119 cm^{-1} for L = corrin,[58] 2124 cm^{-1} for L = octa-ethylporphyrin,[59] 2130 cm^{-1} for L = cobaloxime,[60] and 2134 cm^{-1} for L = [14]aneN$_4$,[61] in exact parallel to the kinetic cis-effect. We therefore expect that as the strength of the interaction between Co(III) and the equatorial macrocyclic ligand increases, ν_{CN} of axially coordinated CN^- will shift to lower frequency.

We have calculated the frequency of the symmetric and antisymmetric stretch of the CN along the series of the C_{10} substituents. The results are reported in Figure 9. The frequencies of the symmetric and antisymmetric stretch are highly correlated ($r^2 = 0.999$; $\Delta\nu_{CN} = 12.3 \pm 0.1$ cm^{-1}) with σ_p for $\sigma_p > 0$, and independent of $\sigma_p < 0$. This is in line with the behavior of the partial charges discussed above; there is therefore also a correlation between the partial charges and ν_{CN}.

As X becomes more electron-withdrawing the ionicity of the NC-Co-CN system decreases and the frequencies move to higher wavenumbers, further from the free cyanide experimental stretching frequency of 2078 cm^{-1} and calculated stretching frequency at the BP86/6-31+G(d,p) level of 2042 cm^{-1}. This suggests that the CN ligand is more constrained and the covalency of the Co−CN increases. This prompted us to examine the nature of the Co−CN bond in our series of structures.

3.5. Electron Density ρ_c at the Co−CN and C≡N Bond Critical Point. There is a direct correlation between the electron density at the bond critical point (bcp), and the strength of a chemical bond as has been demonstrated, for example, for covalent C−C and C−O bonds,[62,63] metal−ligand interactions,[64,65] and hydrogen bonds.[66−69] If we plot ρ_c at the bcp of the Co−CN bond as a function of the σ_p of the C_{10} substituent (Figure 10), we observe that the bond weakens as the electron donor power of the C_{10} substituent increases, in agreement with the charge effects and vibrational trends mentioned before.

dx.doi.org/10.1021/jp304007a | J. Phys. Chem. B 2012, 116, 8836−8845

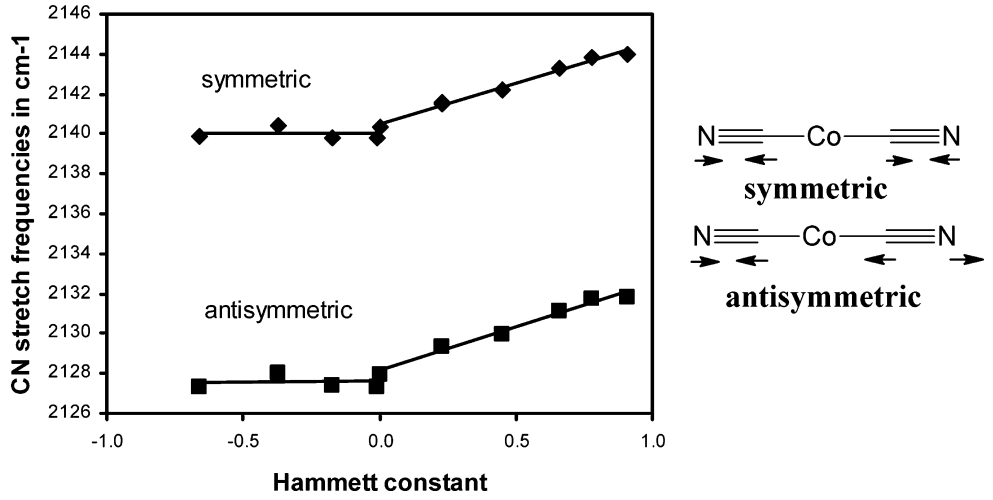

Figure 9. Calculated symmetric and antisymmetric stretching frequency of coordinated cyanide as a function of σ_p of the C_{10} substituent.

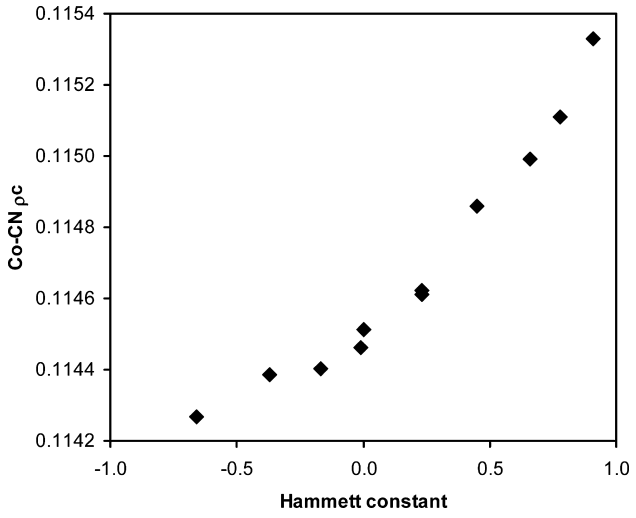

Figure 10. Dependence of the average electron density, ρ_c, at the Co−CN bond critical point on σ_p of the C_{10} substituent.

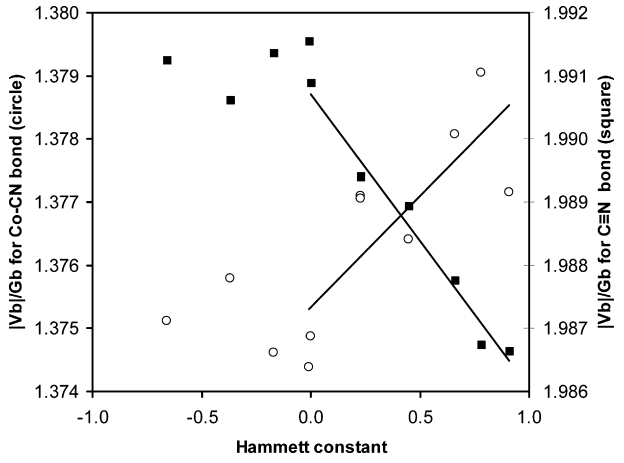

Figure 11. Dependence of the average $|V_b|/G_b$ on σ_p of the C_{10} substituent for the Co−CN bond (○, left axis) and C≡N bond (■, right axis). The linear fittings of the positive part of the Hammett scale are drawn for clarity.

There is very little change, however, in the ρ_c values at the C≡N bond critical point (data not shown).

Espinosa et al.[70] have suggested using the ratio $|V_b|/G_b$ to characterize a bond, where V_b and G_b are the potential and kinetic energy densities at the bcp, respectively. Interactions with $|V_b|/G_b < 1$ are characteristic of closed shell (ionic) interactions; those with $|V_b|/G_b > 2$ are typically shared (covalent) interactions; and $1 < |V_b|/G_b < 2$ are diagnostic of interactions of intermediate character. The dependence of $|V_b|/G_b$ for Co−N and C≡N bonds is plotted in Figure 11. The Co−CN bond in these complexes, by this criterion, is intermediate in character ($1.374 < |V_b|/G_b < 1.380$) whereas the $|V_b|/G_b$ values for the C≡N bonds are close to 2, expected for a covalent interaction.

For both bonds, $|V_b|/G_b$ does not depend on the Hammett constant when $\sigma_p < 0$. For Co−CN $|V_b|/G_b$ increases as with $\sigma_p > 0$, i.e., the Co−CN bond becomes more covalent; conversely, the C≡N bond becomes less covalent and more ionic, in agreement with our observations on the partial charges and the stretching frequencies given above.

4. CONCLUSIONS

By studying very simple cobalt corrin models of the form CN-[Co(III)-corrin]-CN, with DFT and TD-DFT calculations, we have seen that the substitution of H at C_{10} on the corrin ring with electron-donating or electron-withdrawing substituents affects the UV−visible spectrum and the ionicity of the Co-CN bond. We have shown that the position of the α band is more affected than that of the γ band, and there is a linear correlation with the Hammett constant of the C_{10} substituent. The ionicity of the Co−CN bond decreases with the withdrawing power of the C_{10} substituent, the bond is stronger and as a consequence the CN frequency increases. This has implications for understanding the exceptional lability of Co(III) in the cobalt corrins. In results to be reported elsewhere we shall consider the case where the two axial ligands are not the same.

■ AUTHOR INFORMATION

Corresponding Author

*E-mail: Isabelle.Navizet@wits.ac.za; Christopher.Perry2@wits.ac.za.

Notes

The authors declare no competing financial interest.

■ ACKNOWLEDGMENTS

The financial assistance of the Department of Science and Technology, and the National Research Foundation, Pretoria, through the South African Research Chairs Initiative, and the University of the Witwatersrand, Johannesburg, is gratefully acknowledged.

■ REFERENCES

(1) Banerjee, R. *Chemistry and Biochemistry of B_{12}*; John Wiley & Sons, Inc.: New York, 1999.
(2) Marques, H. M.; Knapton, L.; Zou, X.; Brown, K. L. *J. Chem. Soc., Dalton Trans.* **2002**, No. 16, 3195−3200.
(3) Perry, C. B.; Fernandes, M. A.; Brown, K. L.; Zou, X.; Valente, E. J.; Marques, H. M. *Eur. J. Inorg. Chem.* **2003**, *2003* (11), 2095−2107.
(4) Knapton, L.; Marques, H. M. *Dalton Trans.* **2005**, No. 5, 889−895.
(5) Brown, K. L.; Cheng, S.; Zou, X.; Zubkowski, J. D.; Valente, E. J.; Knapton, L.; Marques, H. M. *Inorg. Chem.* **1997**, *36* (17), 3666−3675.
(6) Perry, C. B.; Marques, H. M. *S. Afr. J. Chem.* **2005**, *58*, 9−15.
(7) Brown, K. L. *Chem. Rev.* **2005**, *105* (6), 2075−2149.
(8) Pratt, J. M.; Thorp, R. G. *J. Chem. Soc. A* **1966**, 187−191.
(9) Firth, R. A.; Hill, H. A. O.; Pratt, J. M.; Williams, R. J. P.; Jackson, W. R. *Biochemistry* **1967**, *6*, 2178−2189.
(10) Runge, E.; Gross, E. K. U. *Phys. Rev. Lett.* **1984**, *52*, 997−1000.
(11) Gross, E. K. U.; Ullrich, C. A.; Gossman, U. J. In *Density Functional Theory*; Gross, E. K. U., Dreizler, R. M., Eds.; Plenum Press: New York, 1995.
(12) Grimme, S. In *Reviews in Computational Chemistry*; Lipkowitz, K. B., Larter, R., Cundari, T. R., Eds.; John Wiley & Sons, Inc.: Hoboken, NJ, 2004; Vol. *20*.
(13) Andruniow, T.; Jaworska, M.; Lodowski, P.; Zgierski, M. Z.; Dreos, R.; Randaccio, L.; Kozlowski, P. M. *J. Chem. Phys.* **2008**, *129* (8), 085101.
(14) Andruniow, T.; Jaworska, M.; Lodowski, P.; Zgierski, M. Z.; Dreos, R.; Randaccio, L.; Kozlowski, P. M. *J. Chem. Phys.* **2009**, *131* (10), 105105.
(15) Andruniow, T.; Kozlowski, P. M.; Zgierski, M. Z. *J. Chem. Phys.* **2001**, *115* (16), 7522.
(16) Brooks, A. J.; Vlasie, M.; Banerjee, R.; Brunold, T. C. *J. Am. Chem. Soc.* **2004**, *126* (26), 8167−8180.
(17) Chemaly, S. M.; Brown, K. L.; Fernandes, M. A.; Munro, O. Q.; Grimmer, C.; Marques, H. M. *Inorg. Chem.* **2011**, *50* (18), 8700−8718.
(18) Jaworska, M.; Kazibut, G.; Lodowski, P. *J. Phys. Chem. A* **2003**, *107* (9), 1339−1347.
(19) Kornobis, K.; Kumar, N.; Wong, B. M.; Lodowski, P.; Jaworska, M.; Andruniów, T.; Ruud, K.; Kozlowski, P. M. *J. Phys. Chem. A* **2011**, *115* (7), 1280−1292.
(20) Solheim, H.; Kornobis, K.; Ruud, K.; Kozlowski, P. M. *J. Phys. Chem. B* **2011**, *115* (4), 737−748.
(21) Stich, T. A.; Brooks, A. J.; Buan, N. R.; Brunold, T. C. *J. Am. Chem. Soc.* **2003**, *125* (19), 5897−5914.
(22) Lodowski, P.; Jaworska, M.; Andruniów, T.; Kumar, M.; Kozlowski, P. M. *J. Phys. Chem. B* **2009**, *113* (19), 6898−6909.
(23) Lodowski, P.; Jaworska, M.; Kornobis, K.; Andruniów, T.; Kozlowski, P. M. *J. Phys. Chem. B* **2011**, *115* (45), 13304−13319.
(24) Day, P. *Theor. Chem. Acc.* **1967**, *7* (4), 328−341.
(25) Offenhartz, P. O.; Offenhartz, B. H.; Fung, M. M. *J. Am. Chem. Soc.* **1970**, *92* (10), 2966−2973.
(26) Kozlowski, P. M.; Kumar, M.; Piecuch, P.; Li, W.; Bauman, N. P.; Hansen, J. A.; Lodowski, P.; Jaworska, M. *J. Chem. Theory Comput.* **2012**, *8* (6), 1870−1894.
(27) Bader, R. F. *Atoms in Molecules: A Quantum Theory*; Oxford University Press: Oxford, U.K., 1990.
(28) Frisch, M. J.; Trucks, G. W.; Schlegel, H. B.; Scuseria, G. E.; Robb, M. A.; Cheeseman, J. R.; Scalmani, G.; Barone, V.; Mennucci, B.; Petersson, G. A.; Nakatsuji, H.; Caricato, M.; Li, X.; Hratchian, H. P.; Izmaylov, A. F.; Bloino, J.; Zheng, G.; Sonnenberg, J. L.; Hada, M.; Ehara, M.; Toyota, K.; Fukuda, R.; Hasegawa, J.; Ishida, M.; Nakajima, T.; Honda, Y.; Kitao, O.; Nakai, H.; Vreven, T.; Montgomery, J., J. A.; Peralta, J. E.; Ogliaro, F.; Bearpark, M.; Heyd, J. J.; Brothers, E.; Kudin, K. N.; Staroverov, V. N.; Kobayashi, R.; Normand, J.; Raghavachari, K.; Rendell, A.; Burant, J. C.; Iyengar, S. S.; Tomasi, J.; Cossi, M.; Rega, N.; Millam, N. J.; Klene, M.; Knox, J. E.; Cross, J. B.; Bakken, V.; Adamo, C.; Jaramillo, J.; Gomperts, R.; Stratmann, R. E.; Yazyev, O.; Austin, A. J.; Cammi, R.; Pomelli, C.; Ochterski, J. W.; Martin, R. L.; Morokuma, K.; Zakrzewski, V. G.; Voth, G. A.; Salvador, P.; Dannenberg, J. J.; Dapprich, S.; Daniels, A. D.; Farkas, Ö.; Foresman, J. B.; Ortiz, J. V.; Cioslowski, J.; Fox, D. J. *Gaussian 09*, revision A.02; Gaussian, Inc.: Wallingford, CT, 2009.
(29) Markwell, A. J.; Pratt, J. M.; Shaikjee, M. S.; Toerien, J. G. *J. Chem. Soc., Dalton Trans.* **1987**, No. 6, 1349−1357.
(30) Jensen, K. P.; Ryde, U. *J. Phys. Chem. A* **2003**, *107* (38), 7539−7545.
(31) Kuta, J.; Patchkovskii, S.; Zgierski, M. Z.; Kozlowski, P. M. *J. Comput. Chem.* **2006**, *27* (12), 1429−1437.
(32) Kuta, J.; Wuerges, J.; Randaccio, L.; Kozlowski, P. M. *J. Phys. Chem. A* **2009**, *113* (43), 11604−11612.
(33) Yanai, T.; Tew, D. P.; Handy, N. C. *Chem. Phys. Lett.* **2004**, *393* (1−3), 51−57.
(34) Zhao, Y.; Truhlar, D. *Theor. Chem. Acc.* **2008**, *120* (1), 215−241.
(35) Zhao, Y.; Truhlar, D. G. *Acc. Chem. Res.* **2008**, *41* (2), 157−167.
(36) Becke, A. D. *J. Chem. Phys.* **1993**, *98* (7), 5648−5652.
(37) Lee, C.; Yang, W.; Parr, R. G. *Phys. Rev. B* **1988**, *37* (2), 785.
(38) Stephens, P. J.; Devlin, F. J.; Chabalowski, C. F.; Frisch, M. J. *J. Phys. Chem.* **1994**, *98* (45), 11623−11627.
(39) Vosko, S. H.; Wilk, L.; Nusait, M. *Can. J. Chem.* **1980**, *58* (8), 1200−1211.
(40) Adamo, C.; Barone, V. *J. Chem. Phys.* **1999**, *110* (13), 6158−6170.
(41) Perdew, J. P.; Burke, K.; Ernzerhof, M. *Phys. Rev. Lett.* **1996**, *77* (18), 3865−3868.
(42) Perdew, J. P.; Burke, K.; Ernzerhof, M. *Phys. Rev. Lett.* **1997**, *78* (7), 1396−1396.
(43) http://www.chemcraftprog.com; Chemcraft software.
(44) Biegler-König, F. W.; Schönbohm, J.; Bayles, D. *AIM2000*, 1; http://www.gauss.fh-bielefeld.de/aim2000.
(45) Keith, T. A. *AIMAll*, 08.05.04; http://aim.tkgristmill.com, 2008.
(46) Eschenmoser, A.; Scheffold, R.; Bertele, E.; Pesaro, M.; Gschwend, H. *Proc. R. Soc. London, A* **1965**, *288* (1414), 306−323.
(47) Wagner, F. *Proc. R. Soc. London A* **1965**, *A228*, 344−347.
(48) Wagner, F.; Bernhauer, K. *Ann. N.Y. Acad. Sci.* **1964**, *112*, 580−589.
(49) Neese, F. *J. Biol. Inorg. Chem.* **2006**, *11*, 702−711.
(50) Sension; Harris; Stickrath; Cole; Fox; Marsh. *J. Phys. Chem. B* **2005**, *109*, 18146−18152.
(51) Hansch, C.; Leo, A.; Taft, R. W. *Chem. Rev.* **1991**, *91*, 165−195.
(52) Nakagawa, I.; Shimanouchi, T. *Spectrochim. Acta* **1962**, *18*, 101−113.
(53) Dunbar, K. R.; Heintz, R. A. *J. Am. Chem. Soc.* **1988**, *110*, 8247−8249.
(54) Dunbar, K. R.; Heintz, R. A. In *Progress in Inorganic Chemistry*; Karlin, K. D., Ed.; John Wiley & Co.: New York, 1997; Vol. *45*, pp 283−391.
(55) Tsubaki, M.; Yoshikawa, S. *Biochemistry* **1993**, *32*, 164−173.
(56) Boffi, A.; Chiancone, E.; Takahashi, S.; Rousseau, D. L. *Biochemistry* **1997**, *36*, 4505−4509.
(57) Pratt, J. M. *The Inorganic Chemistry of Vitamin B_{12}*; Academic Press: London, 1972.
(58) Firth, R. A.; Hill, H. A. O.; Pratt, J. M.; Thorp, R. G.; Williams, R. J. P. *J. Chem. Soc. A* **1968**, 2428−2433.
(59) Fahmy, N.; Leverenz, A.; Hanack, M. *Synth. Met.* **1991**, *41*−*43*, 2615−2619.
(60) Dodd, D.; Johnson, M. D. *J. Chem. Soc., Dalton Trans.* **1973**, 1218−1226.
(61) Watzky, M. A.; Endicott, J. F.; Song, X.; Lei, Y.; Macatangay, A. *Inorg. Chem.* **1996**, *35*, 3463−3473.

(62) Howard, S. T.; Krygowski, T. M. *Can. J. Chem.* **1997**, *75*, 1174−1181.
(63) O'Brien, S. E.; Popelier, P. L. *Can. J. Chem.* **1999**, *77*, 28−36.
(64) Bader, R. F. W.; Matta, C. F.; Cortés-Guzmán, F. *Organometallics* **2004**, *23*, 6253−6263.
(65) Vidal, I.; Melchor, S.; Alkorta, I.; Elguero, J.; Sundberg, M. R.; Dobado, J. A. *Organometallics* **2006**, *25*, 5638−5647.
(66) González, L.; Mó, O.; Yáñez, M.; Elguero, J. *J. Mol. Str.* **1996**, *371*, 1−10.
(67) Espinosa, E.; Souhassou, M.; Lachekar, H.; Lecomte, C. *Acta Cryst. B* **1999**, *55*, 563−572.
(68) Grabowski, S. J. *J. Phys. Chem. A* **2000**, *105*, 5551−5557.
(69) Sobczyk, L.; Grabowski, S. J.; Krygowski, T. M. *Chem. Rev.* **2005**, *105*, 3513−3560.
(70) Espinosa, E.; Alkorta, I.; Elguero, J.; Molins, E. *J. Chem. Phys.* **2002**, *117*, 5529−5542.